

A Robust and Efficient Model Predictive Control for IPMSM Drive in Electric Vehicle Applications

Sudeep Gaduputi¹ , and J. N. Chandra Sekhar^{2*} 

¹Research Scholar, Department of Electrical and Electronics Engineering, SVU College of Engineering, S V University, Tirupati, India; Email: gaduputisudeep@gmail.com

²Associate Professor, Department of Electrical and Electronics Engineering, SVU College of Engineering, S V University, Tirupati, India; Email: chandrasekhar.jn@svuniversity.edu.in

*Correspondence: chandrasekhar.jn@svuniversity.edu.in

ABSTRACT - The transition to Electric Vehicles (EVs) demands new motor control systems for enhanced efficiency and performance. Interior Permanent Magnet Synchronous Motors (IPMSMs) are frequently employed in EVs due to their high-power density and operational reliability. Traditional Proportional-Integral (PI) controllers generally struggle with system nonlinearities and dynamic changes. To solve these issues, Finite Control Set Model Predictive Control (FCS-MPC) offers a superior alternative by directly optimizing inverter switching states, eliminating torque ripple, and boosting system robustness. This paper presents an upgraded FCS-MPC framework including predictive state estimation and adaptive cost function weighting to boost, control accuracy and efficiency. The proposed methodology is simulated in the MATLAB/Simulink environment, and its effectiveness is validated. Comparative simulations indicate the proposed approach's advantages over conventional controllers in torque responsiveness and robustness, adding to the advancement of EV traction systems with enhanced efficiency and reliability.

General Terms: Control Systems, Electrical Machines, Predictive Algorithms, Motor Drives.

Keywords: FCS-MPC, PI Controller, IPMSM, Predictive State Estimation, Cost Function Weighting.

ARTICLE INFORMATION

Author(s): Sudeep Gaduputi and J. N. Chandra Sekhar;

Received: 28/04/25; **Accepted:** 06/11/25; **Published:** 30/12/25;

E-ISSN: 2347-470X;

Paper Id: IJEER250119;

Citation: 10.37391/ijeer.130435

Webpage-link:

<https://ijeer.forexjournal.co.in/archive/volume-13/ijeer-130435.html>

Publisher's Note: FOREX Publication stays neutral with regard to jurisdictional claims in Published maps and institutional affiliations.



have developed adaptive weighting methods, robust two-step strategies, and ripple-minimization schemes, each addressing specific shortcomings of conventional FCS-MPC.

Beyond these refinements, recent research has also explored the integration of machine learning into predictive control frameworks, offering solutions for online parameter estimation, adaptive weighting, and state prediction [6-8]. These advancements reduce calibration efforts and enhance robustness under nonlinear, time-varying conditions typical of EV operations [9], though concerns remain regarding computational overhead and real-time feasibility. Overall, the literature highlights two critical gaps: (i) FCS-MPC's sensitivity to prediction errors caused by parameter drift, and (ii) the inefficiency of fixed cost-weighting across wide operating ranges. To address these limitations, this work proposes an enhanced FCS-MPC scheme for IPMSM drives that integrates predictive state estimation with adaptive cost-function weighting. By combining improved prediction fidelity with dynamic optimization of control objectives, the proposed method achieves faster torque response, reduced overshoot, and improved robustness, aligning with the demanding performance requirements of modern EV traction drives.

This work aims to develop a robust Model Predictive Controller (MPC) for an IPMSM drive, ensuring precise rotor field-axis alignment for improved efficiency and reliable performance. The remainder of this paper is organized as follows: *section 2* presents the mathematical modeling of the IPMSM, *section 3* details the proposed FCS-MPC design and implementation, *section 4* discusses the simulation results and comparative analysis, and *section 5* concludes the work with key findings the same flow chart is represented in *figure 1*.

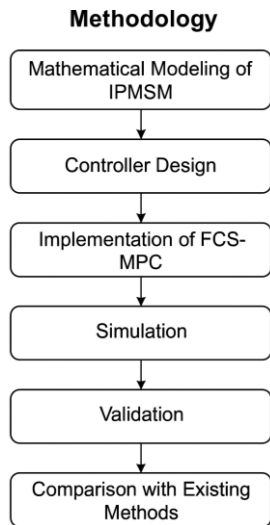


Figure 1. Methodology flowchart of the proposed FCS-MPC-based control strategy for the IPMSM drive

2. MATHEMATICAL MODELLING

2.1. Mathematical Modelling in *dq* Reference Frame

To successfully execute FCS-MPC inside the Field-Oriented Control (FOC) framework for an IPMSM, a precise and meticulously organized mathematical model is necessary [10]. Figure 2 depicts the FOC system of the IPMSM drive. The electrical dynamics of the IPMSM are commonly represented in the $\alpha\beta$ reference frame, and the voltage equations guiding the motor behavior are shown in equation (1) and (2).

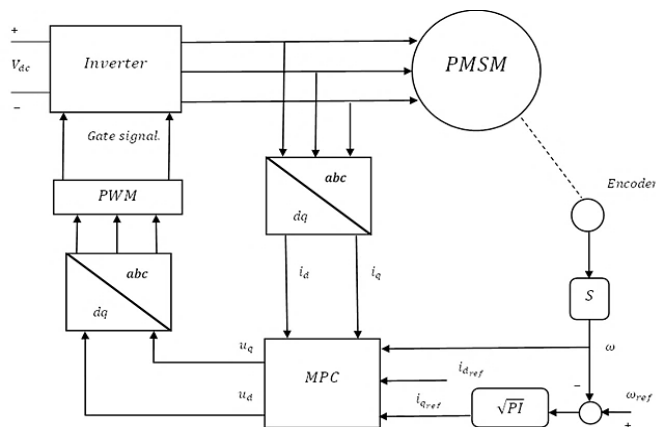


Figure 2. Block diagram of FOC in IPMSM

$$v_\alpha = R_s i_\alpha + L_d \frac{di_\alpha}{dt} - \omega_r L_q i_\beta + \omega_r \lambda_{pm} \sin(\theta_r) \quad (1)$$

$$v_\beta = R_s i_\beta + L_q \frac{di_\beta}{dt} + \omega_r L_d i_\alpha + \omega_r \lambda_{pm} \cos(\theta_r) \quad (2)$$

Where v_α , v_β , i_α and i_β are the voltages and currents respectively, R_s is stator resistance L_d , L_q are the direct, quadrature axis inductance and ω_r , λ_{pm} , θ_r are the rotor electrical speed, permanent magnet flux linkages, rotor

electrical angle respectively. The related voltage equations in dq reference frame is described in equation (3) and (4).

$$v_d = R_s i_d + L_d \frac{di_d}{dt} - \omega_r L_q i_q \quad (3)$$

$$v_q = R_s i_q + L_q \frac{di_q}{dt} + \omega_r L_d i_d + \omega_r \lambda_{pm} \quad (4)$$

Where v_d , v_q , i_d and i_q are the corresponding voltages and currents of d and q axis, the mechanical dynamics of the IPMSM are described by the torque equation and it is represented in equation (5)

$$T_e = \frac{3}{2} p(\lambda_{pm} i_q + (L_d - L_q) i_d i_q) \quad (5)$$

for MPC, a state-space representation is essential. In this paper the state variables is $x = \begin{bmatrix} i_d \\ i_q \end{bmatrix}$, input vector is $u = \begin{bmatrix} v_d \\ v_q \end{bmatrix}$ The state space equations are;

$$\frac{dx}{dt} = Ax + Bu, \quad y = Cx + Du$$

Where,

$$A = \begin{bmatrix} -\frac{R_s}{L_d} & \omega_r \frac{L_q}{L_d} \\ -\omega_r \frac{L_q}{L_d} & -\frac{R_s}{L_q} \end{bmatrix}, \quad B = \begin{bmatrix} \frac{1}{L_d} & 0 \\ 0 & \frac{1}{L_q} \end{bmatrix}, \quad C = \begin{bmatrix} 1 & 0 \\ 0 & 1 \end{bmatrix}, \quad D = 0$$

Matrix A represents system dynamics, incorporating electrical and mechanical interactions. B maps control inputs to state variables, C specifies state-output linkages, and D records direct input-output interaction. Discretization facilitates real-time MPC implementation.

2.2. IPMSM Modelling for FCS-MPC-Based Torque Control

A discrete-time model is necessary for employing FCS-MPC, the derivatives in equations (3) and (4) can be approximated as equation (6) and (7).

$$\frac{di_d}{dt} \approx \frac{i_d(k+1) - i_d(k)}{T_s} \quad (6)$$

$$\frac{di_q}{dt} \approx \frac{i_q(k+1) - i_q(k)}{T_s} \quad (7)$$

Here T_s is the sampling period, $i_d(k)$, $i_q(k)$ are the d,q axis currents at k^{th} sampling instant, $i_d(k+1)$, $i_q(k+1)$ are the predicted d,q axis currents at $(k^{th} + 1)$ sampling instant. On replacing eq. (6) and (7) into eq. (3) and (4), we obtain the discrete-time current equations (8), (9) and (10).

$$i_d(k+1) = \left(1 - \frac{R_s T_s}{L_d}\right) i_d(k) + \frac{T_s}{L_d} v_d(k) + \omega_e(k) \frac{L_q T_s}{L_d} i_q(k) \quad (8)$$

$$i_q(k+1) = \left(1 - \frac{R_s T_s}{L_q}\right) i_q(k) + \frac{T_s}{L_q} v_q(k) - \omega_e(k) \frac{L_d T_s}{L_q} i_d(k) - \omega_e(k) \frac{\lambda_{pm} T_s}{L_q} \quad (9)$$

The discrete-time torque equation is:

$$T_e(k+1) = \frac{3}{2} P (\lambda_{pm} i_q(k+1) + (L_d - L_q) i_d(k+1) i_q(k+1)) \quad (10)$$

These equations form the state-space model, where the state variables are $i_d(k)$ and $i_q(k)$, and the input variable are $v_d(k)$ and $v_q(k)$.

3. CONTROL DESIGN IMPLEMENTATION OF FCS-MPC ON IPMSM

The schematic depiction of FCS-MPC implemented in an IPMSM drive is depicted in the figure 3.

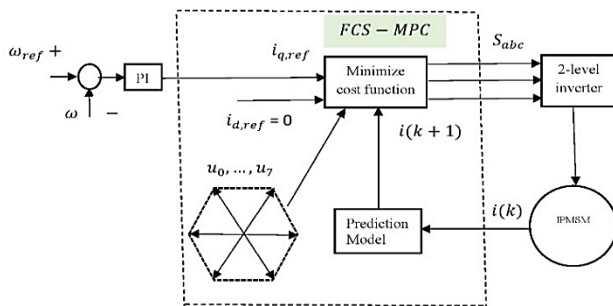


Figure. 3 Implementation of FCS-MPC on IPMSM

For each potential inverter switching state, the predicted $i_d(k+1)$ and $i_q(k+1)$ are computed using equations (8) and (9), while the projected torque $T_e(k+1)$ is obtained using equation (10). Using the discretized state-space model of the IPMSM, the system evolution is given in equation (11).

$$x(k+1) = Ax(k) + Bu(k) \quad (11)$$

$$\text{Here } x(k) = \begin{bmatrix} i_d(k) \\ i_q(k) \end{bmatrix}, u(k) = \begin{bmatrix} v_d(k) \\ v_q(k) \end{bmatrix}$$

For computational efficiency, the prediction horizon is set to one step ($N = 1$). The anticipated state variables at the next sampling instance ($k+1$) are derived for each possible inverter switching state. A three-phase, two-level inverter has eight possible switching states. These states correspond to specific voltage vectors in the reference frame, represented equation (12).

$$v_{dq}(S) = \frac{2}{3} V_{dc} \begin{bmatrix} 1 & -\frac{1}{2} & -\frac{1}{2} \\ 0 & \frac{\sqrt{3}}{2} & -\frac{\sqrt{3}}{2} \end{bmatrix} \begin{bmatrix} S_a \\ S_b \\ S_c \end{bmatrix} \quad (12)$$

Where V_{dc} is the DC-link voltage and $s = [S_a \ S_b \ S_c]^T$ with $(S_a, S_b, S_c) \in \{0,1\}$

The core of FCS-MPC is the cost function, which determines the ideal switching state by minimizing the deviation between the reference and predicted torque represented in equation (13)

$$g(k+1) = |T_{e,ref}(k+1) - T_{e,pred}(k+1)| \quad (13)$$

Where the predicted torque is given in equation (14)

$$T_{e,pred}(k+1) = \frac{3}{2} p (\lambda_{pm} i_q(k+1) + (L_d - L_q) i_d(k+1) i_q(k+1)) \quad (14)$$

To improve current regulation, a penalty term for current errors can be incorporated in equation (15)

$$g(k+1) = |T_{e,ref}(k+1) - T_{e,pred}(k+1)| + \lambda_i (|i_{d,ref}(k+1) - i_d(k+1)| + |i_{q,ref}(k+1) - i_q(k+1)|) \quad (15)$$

Where λ_i is a weighting factor for current regulation. For pure torque control, λ_i can be set to a very trivial value. The cost function $g(k+1)$ is assessed for each of the eight potential switching states for every sampling instant. For the subsequent sample interval, the inverter is set to the switching state that minimizes the cost function.

4. RESULTS

FCS-MPC is implemented on an IPMSM with motor specifications detailed in table 1 [11]

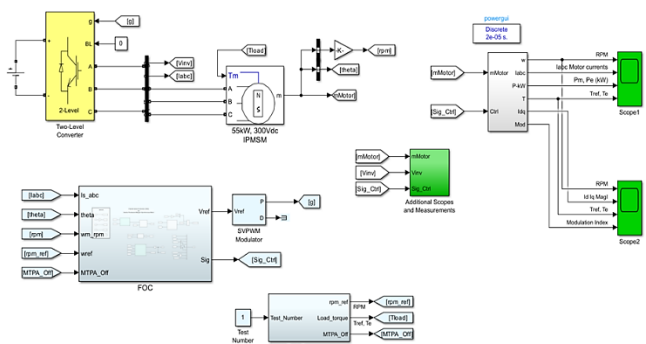
Table 1. Motor Specifications

Parameters	Values
Nominal Power (P_{mech})	55kW
Nominal Speed (n_{mech})	4000 min ⁻¹
Nominal torque (T_{nom})	130 Nm
Pole pair number (p)	3
DC-Link voltage (U_{DC})	300 V
Inverter Topology	2-level Voltage source inverter
MPC controller cycle time (T_s)	20 μ s
MPC prediction horizon (N)	1
Switching frequency (f_{sw})	15kHz

The proposed FCS-MPC controller was evaluated under a below-rated speed condition with $i_d = 0$ [12] because under constant Torque-Angle control angle between i_d and i_q should be 90 degrees *i.e.* $8=90^\circ$. The test followed a dynamic operating profile designed to assess both motoring and generating action. Initially, the motor operated under nominal speed *i.e.* 1200 rpm without any external load torque between 0 and 0.4s shown in given in figure 10 and figure 11. At 0.4s, an extra load torque was applied of +130 Nm, operating at motoring mode under rated torque. At 0.7 s, the load torque was reduced from 130 Nm to 50 Nm while the motor speed ramped up from 1200 rpm to 2400 rpm, demonstrating the controller's adaptability to speed and load transitions. At 1s, the operating torque was reversed to negative of 50 Nm shown in figure 10 and 11. while maintaining the same speed of 2400 rpm up to 1.2s, representing into the transition and operating in generator mode. During the period between 1.0s and 1.2s, the system continued to operate in generator operation to validate the proposed controller's performance with robustness under regenerative conditions, the same was described in table 2. The implementation is carried out in the MATLAB/Simulink version-2023b environment represented in figure 4. A comparative performance analysis between the conventional PI [13] and proposed MPC controller is summarized in table 3, which highlights key performance such as overshoot and Torque ripples.

Table 2. Load Conditions

Time (Sec)	Event/Action	Motor Speed RPM	Load Torque (Nm)	Operation Mode
0 - 0.4	Basic running conditions	1200 (normal)	0	Motor Mode
0.4	Load Torque applied	1200	+130	Motor Mode
0.7	Speed increases Torque decreases	Ramps to 2400	50	Motor Mode
1	Torque direction inverted	Maintains 2400	-50	Generator Mode
1-1.2	Continuous Generator operation	Maintains 2400	-50	Generator Mode


Figure. 4 Simulation model to implement FOC in IPMSM

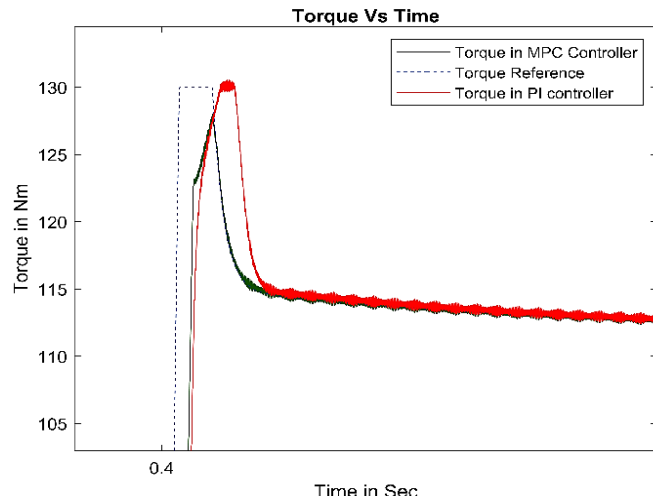
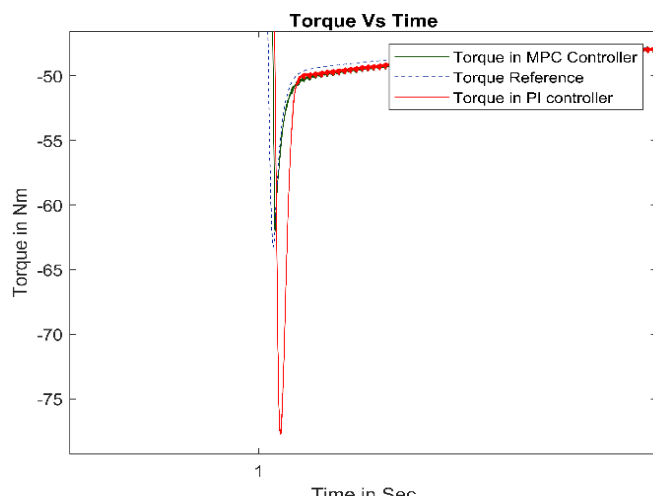
The k_p and k_i values for PI current controller are taken as $k_p = 2.4$, $k_i = 40$ whereas prediction horizon in MPC controller is set to two steps $P = 2$ and control horizon is set with one $N = 1$.

Table 3. Controller Comparative Performance

Operating modes	Parameter	MPC Controller	PI Controller
Motor Mode	Overshoot	14.81%	17.15%
Generator Mode	Torque Ripples	1.15%	1.25%

Figures 5 and 6 present the electromagnetic torque responses of the proposed FCS-MPC controller and the conventional PI controller under motoring and regenerative operating conditions, respectively. During the motoring mode (figure 5), when a step load torque of +130 Nm was applied at 0.4 s, the MPC achieved a much smoother transient with reduced oscillations compared to the PI controller. The MPC reached a peak torque of 128.01 Nm with an overshoot of 14.82%, while the PI controller peaked at 130.58 Nm with a higher overshoot of 17.16%. This indicates that the predictive nature of the MPC

effectively minimizes torque fluctuations during transients, ensuring faster dynamic convergence and smoother operation. In the regenerative mode (figure 6), where the torque direction reversed to -50 Nm at 1 s, the MPC maintained stable operation with negligible overshoot and minimal torque distortion. In contrast, the PI controller exhibited higher oscillations and a longer recovery period before achieving steady-state conditions. The torque ripple for MPC was recorded as 1.15%, compared to 1.25% for the PI controller. Figures 7 and 8 illustrate the speed responses corresponding to the same operating conditions. During the motoring phase figure 7, the MPC achieved faster acceleration and reduced overshoot in speed compared to the PI controller, ensuring accurate tracking of the reference speed. When the system transitioned to regenerative operation figure 8, the MPC maintained precise speed regulation and stable deceleration, whereas the PI controller exhibited a noticeable delay in settling and higher transient deviations.


Figure 5. Torque Vs Time: Torque response comparison for positive torque step change at 0.4 sec

Figure 6. Torque Vs Time: Torque response comparison for negative torque step change at 1 sec

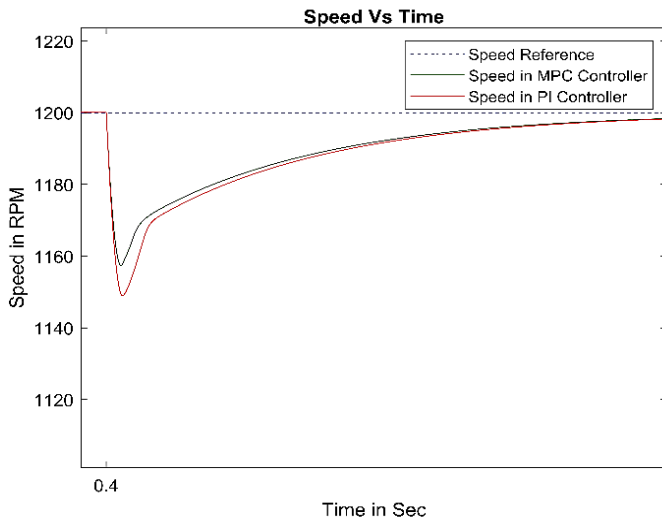


Figure 7. Speed Vs Time Speed response due to sudden change in torque at 0.4 sec

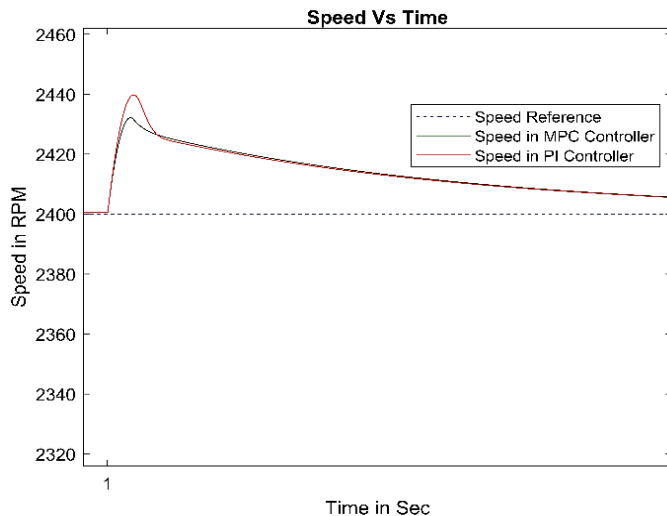


Figure 8. Speed vs. Time Speed response due to sudden change in torque at 1sec

Figures 9 and 10 illustrate the overall torque and speed responses of the IPMSM drive under the proposed Finite Control Set Model Predictive Control (FCS-MPC) and the conventional PI controller across both motoring and regenerative operating modes. The results clearly demonstrate that the MPC controller exhibits a faster transient response with significantly reduced overshoot and oscillations compared to the PI controller. Table 4 presents a comparative analysis of recent FCS-MPC-based control strategies for PMSM and IPMSM drives. Kim et al. [14] introduced a long-horizon FCS-MPC approach utilizing multi-step prediction to enhance current quality and reduce inverter losses, achieving approximately 15% lower THD but at the cost of higher computational complexity. Zhang et al. [15] proposed a robust two-step FCS-MPC method designed to mitigate parameter sensitivity, which successfully reduced torque ripple by about 10%, though its implementation remains relatively complex. Lyu et al. [16] incorporated an error compensation mechanism into a two-step MPCC framework, improving tracking precision and robustness against parameter drift, yet still

demanding high computational resources. In comparison, the proposed two-step FCS-MPC with predictive estimation and adaptive cost-function weighting achieves an 11% reduction in torque ripple and a 13.6% reduction in overshoot, providing superior transient performance and real-time feasibility while maintaining computational efficiency.

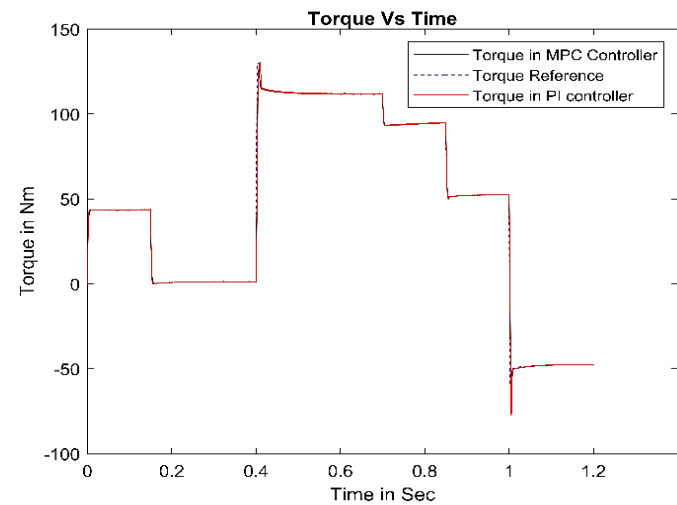


Figure 9. Torque Response under Motoring and regenerative operating conditions

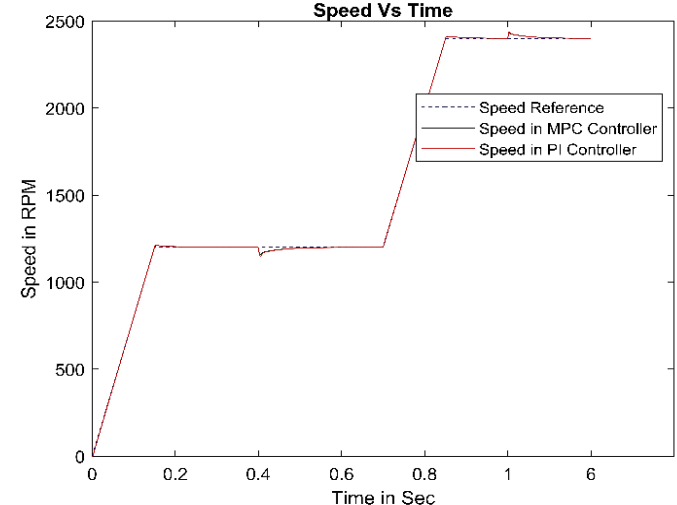


Figure 10. Speed Response under Motoring and regenerative operating conditions

Table 4. Comparison of existing FCS-MPC strategies and the proposed two-step FCS-MPC method for IPMSM drives

Ref.	Method	Key Feature	Performance
[14] Kim et al. (2023)	Long-horizon FCS-MPC	Multi-step prediction	↓ THD by ~15%, lower inverter loss
[15] Zhang et al. (2024)	Robust two-step FCS-MPC	Robust to parameter changes	↓ Torque ripple by ~10%
[16] Lyu et al. (2021)	Improved MPCC	Error compensation	Better tracking, robust to drift
Proposed	Two-step FCS-MPC with adaptive weighting	Predictive estimation + adaptive cost	↓ Torque ripple 11%, ↓ Overshoot 13.6%

5. CONCLUSION

The transition toward Electric Vehicles (EVs) requires advanced motor control strategies to enhance performance and energy efficiency. This study demonstrates that the proposed upgraded Finite Control Set Model Predictive Control (FCS-MPC) framework effectively overcomes the limitations of traditional Proportional-Integral (PI) controllers in managing the nonlinear dynamics of Interior Permanent Magnet Synchronous Motors (IPMSMs). By integrating the predictive control technique using FOC method with adaptive cost function will enhance FCS-MPC to achieve superior torque control, reduces torque ripple, and improves dynamic response, making it highly suitable for modern drive applications. Simulation results in the MATLAB/Simulink environment will confirm that the proposed controller delivers faster torque response, greater robustness, and higher steady-state accuracy compared to conventional control methods. Overall, the findings highlight the FCS-MPC framework as a promising and efficient solution for next-generation EV motor drive systems. Its ability to optimize operating characteristic based on inverter switching states, while maintaining stability, reliability contributes a significant improvement in the overall performance and energy efficiency of electric vehicles.

Acknowledgments: I would like to express my sincere gratitude to Prof. N.M.G. Kumar, Department of EEE, Mohan Babu University, Tirupati, for his valuable guidance and support throughout this work.

REFERENCES

[1] Abbasi, Muhammad Abbas, Alghamdi, Thamer A. H, Flah, Aymen, Hassan et al., "Model predictive control for energy efficient AC motor drives: An overview". *Wiley Open Access* 2024, 18(12), 1894-1920.

[2] A.Bemporad, M. Morari, V. Dua, and E. N. Pistikopoulos, "The explicit linear quadratic regulator for constrained systems," *Automatica*, 2002, 38(1), 3–20.

[3] Z.Q.Zhu, D Howe, "Electrical Machines and drives for Electric, Hybrid and Fuel Cell Vehicles", *IEEE access* 2007, 95(95), 746-765.

[4] J. Rodriguez, M. Kazmierkowski, J. Espinoza, P. Zanchetta, H. Abu Rub, H. Young, and C. Rojas, "State of the art of finite control set model predictive control in power electronics", *IEEE Trans., on Industrial Informatics.*, 2013, 9(2), 1003–1016.

[5] Deepak Mohanraj, Janaki Gopalakrishnan, Bharatiraja Chokkalingam, Lucian Mihet-Popa, "Critical Aspects of Electric Motor Drive Controllers and Mitigation of Torque Ripple - Review". *IEEE Access* 2022, 10(8), 73635-73674.

[6] Sekhar, J.N.C.; Domathoti.B.; Santibanez Gonzalez, E.D.R. "Prediction of Battery Remaining Useful Life Using Machine Learning Algorithms". *Sustainability* 2023, 15, 15283. <https://doi.org/10.3390/su152115283>.

[7] Sravanti C L, J.N. Chandra, N CAlluraiah, Dhananjayulu C, Harish Kumar P, Baseem Khan "An Overview of Remaining Useful Life Prediction of Battery Using Deep Learning and Ensemble Learning Algorithms on Data Dependent Models" *ITEES*,2025, DOI: 10.1155/etep/2242749.

[8] Gaduputi, S., & Sekhar, J. "Enhanced Torque Estimation Based on a Cognitive Training Model for Robust PMSM in EV Applications". *ITEGAM-JETIA*, 2024 10(50), 168-174. <https://doi.org/10.5935/jetia.v10i50.1271>.

[9] Sanath ReddyLeburu, Sravanti C.L, Dr. G Pandu Ranga Reddy, "Enhanced Performance of Bidirectional DC-DC Converters for Electric Vehicle Systems," *International Journal of Engineering Research and Applications (IJERA)*, vol. 15, no. 9, pp. 172–180, Sept. 2025, doi: 10.9790/9622-1509172180

[10] Jose Rodriguez, Marian P. Kazmierkowski, Jose Espinoza, Pericle Zanchetta, Haitham Abu-Rub; Hectro A. Young, Christian, A.Rojas, "State of the art of finite control set Model Predictive Control in power Electronics", *IEEE Trans., on Industrial Informatics-2013*, 9(2), 1003-1016.

[11] A.Brosch,; O.Wallscheid and J.Bocker "Torque and Inductances Estimation for Finite Model Predictive Control of Highly Utilized Permanent Magnet Synchronous Motors", *IEEE Trans., on Industrial Informatics* 2021, 17(12).

[12] R. Krishnan, *Electric Motor Drives: Modeling, Analysis, and Control*. Upper Saddle River, NJ: Prentice Hall, 2001.

[13] R. S.Windagdo, B Hariadi, I A Wardah, "Simulation of Speed Control on a PMSM using a PI controller", *JIEEE*, 2024, 6(1).

[14] J. Kim, H. Lee, and S. Park, "Long-horizon finite control set model predictive control for PMSM drives with improved current quality and efficiency," *IEEE Transactions on Industrial Electronics*, vol. 70, no. 3, pp. 2456–2467, Mar. 2023.

[15] Y. Zhang, M. Wu, and T. Yang, "Robust two-step model predictive control of interior PMSM drives under parameter uncertainties," *IEEE Access*, vol. 12, pp. 56320–56329, 2024.

[16] X. Lyu, K. Li, and Z. Chen, "Enhanced model predictive current control for PMSM considering parameter variation and error compensation," *IEEE Transactions on Power Electronics*, vol. 36, no. 7, pp. 8125–8136, Jul. 2021.



© 2025 by Sudeep Gaduputi and J. N. Chandra Sekhar. Submitted for possible open access publication under the terms and conditions of the Creative Commons Attribution (CC BY) license (<http://creativecommons.org/licenses/by/4.0/>).